Application of 3-Quinolinoyl Picket Porphyrins to the Electroreduction of Dioxygen to Water: Mimicking the Active Site of Cytochrome *c* Oxidase

David Ricard,[a] Amandine Didier,[a] Maurice L'Her,[b] and Bernard Boitrel*[a]

KEYWORDS:

cytochrome *c* oxidase · electrochemistry · heme proteins · oxidoreductases · O – O activation

Cytochrome *c* oxidase (C*c*O), the terminal enzyme of the respiratory chain, performs the $4e^-$ reduction of dioxygen to water in the mitochondria. This reaction is coupled with proton translocation across the membrane. The energy released by this process is used to convert ADP into ATP. The so-called Fe_{a3}-Cu_B binuclear active site of this enzyme reduces dioxygen to water without any leaking of partially reduced intermediates, such as hydrogen peroxide, which are toxic for the cell (Figure 1).[1] Despite all efforts to elucidate the mechanism of dioxygen reduction to water, different aspects remain controversial, such as the nature of the O_2-bound intermediate or the role of Cu_B and Tyr 244 on the distal side of the porphyrin core. For example, resonance Raman spectroscopic studies initiated by CO photolysis have led to a putative mechanism of the electroreduction of O_2 to H_2O involving an initial myoglobin-like $Fe-O_2$ binding mode, a peroxo-, a ferryl-, and finally a hydroxy intermediate.[2]

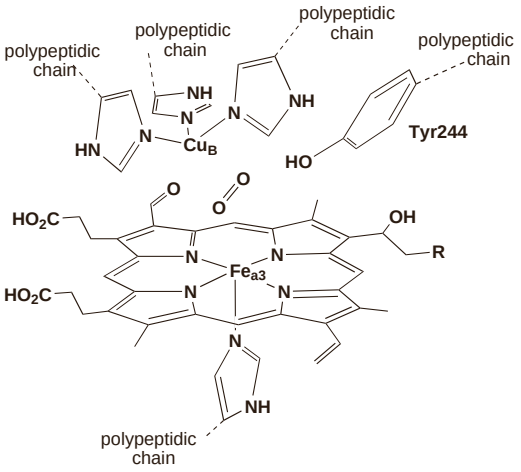

Figure 1. *Schematic representation of the binuclear $Fe_{a3}-Cu_B$ active site of CcO.*

[a] *Dr. B. Boitrel, Dr. D. Ricard, A. Didier*
Université de Bourgogne/LSEO
UMR-CNRS 5632
B.P. 138, 6 boulevard Gabriel, 21000 Dijon (France)
Fax: (+33) 3-80-39-61-14
E-mail: bboitrel@satie.u-bourgogne.fr

[b] *Dr. M. L'Her*
Université de Bretagne Occidentale
Faculté des Sciences, UMR-CNRS 6521
B.P. 809, 29285 Brest Cedex (France)

The determination of two X-ray crystal structures[3] in 1995 opened the way to a new generation of models.[4] However, the exact nature of the peroxo species (hydroperoxo or μ-peroxo with Cu_B) remains uncertain. For these reasons, we have developed a series of models and tried to determine the precise role of each individual component in the mechanism of C*c*O. Special attention is given to the exact role of Cu_B in the natural enzyme and the nature of the peroxo species formed during the catalytic reaction. In a previous paper about iron-only "Arbor" porphyrins, which are tren-capped iron porphyrins (tren = tris(2-aminoethyl)amine) with an external axial base bound to the iron center on the other side of the porphyrin core, we have pointed out that these compounds, with no copper ligated to the tren moiety, are efficient catalysts for the $4e^-$ electroreduction of dioxygen to water.[4c] This observation, excluding the formation of the μ-peroxo iron – copper species as the key step of the catalytic cycle, led us to design new structural and functional models structurally closer to the active site to find out if this property could be observable with other biomimetic models. Here we report our results about the synthesis and the electrocatalytic activity of quinolinoyl picket porphyrins with or without copper in the distal side of the porphyrin and also with either a tailed or an external nitrogen base to stabilize the iron(II) ion as a five-coordinate complex. To our knowledge, this is the first time that such systematic comparisons have been carried out. A significant amount of work has already focused on related compounds but, most of the time, three crucial points did not receive enough attention: a) The catalytic efficiency of the reported compounds toward the reduction of O_2 to water was not always tested; most of them were designed only as model compounds for spectroscopic investigations; b) The structural requirements to mimic the natural function, such as the presence of nitrogen atoms that are part of an aromatic system to stabilize the copper ion in its coordination site and the off-centering between the two metal centers, were sometimes neglected. c) The prevention of any intermolecular reaction on the distal side of the porphyrin between two copper ions was not always taken into account. Indeed, the new copper-binding domain introduced by the three quinolinoyl moieties might satisfy these three major requirements. The three quinolinoyl pickets should impose an obvious off-centering between the two metal centers tethered at a fixed length, whereas the encumbered quinolines should effect a real protection of the distal side of the porphyrin, which is achieved by the polypeptidic chain in the enzyme (Scheme 1). In addition, compounds **4** and **5** contain a covalently bound imidazole group as the fifth ligand on the opposite side of the copper-binding domain. Indeed, the fourth position of substitution on the porphyrin has been used to graft a tailed base to probe its effect on the catalytic activity.

The synthetic route to the final Fe – Cu complexes **3c** and **5c** is outlined in Scheme 1. The $\alpha,\alpha,\alpha,\alpha$ atropisomer[13] of the *meso*-(tetra-*o*-aminophenyl)porphyrin (TAPP)[5] is singly acetylated

  1439-4227/01/02/02 $ 17.50+.50/0

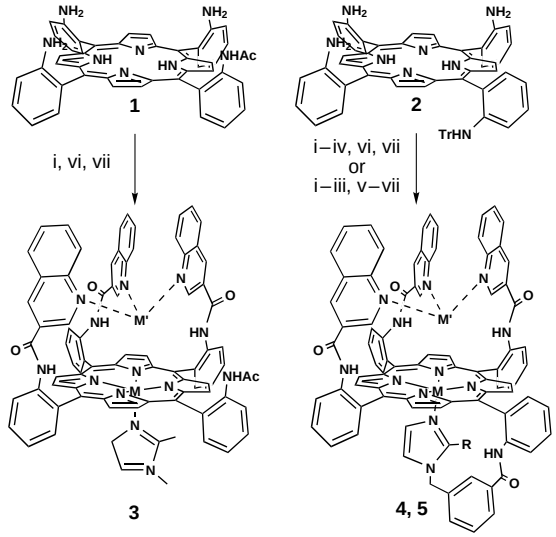

	M	M'
3a	2H	–
3b	Fe	–
3c	Fe	CuBr

	M	M'	R
4a	2H	–	H
4b	Fe	–	H
5a	2H	–	Me
5b	Fe	–	Me
5c	Fe	CuBr	Me
5d	Cu	–	Me

Scheme 1. *Synthesis of iron(II) – copper(I) quinolinoyl picket porphyrins. i) 3-quinoline acyl chloride, NEt_3, THF; ii) TFA, CH_2Cl_2; iii) 3-chloromethylbenzoyl chloride, NEt_3, THF; iv) Im, NaI, THF, 55 °C, N_2, darkness; v) 2-MeIm, NaI, THF, 55 °C, N_2, darkness; vi) $FeBr_2$, 2,6-lutidine, THF, 55 °C; vii) CuBr, CH_3CN, 80 °C. Im = imidazole; Tr = trityl = triphenylmethyl.*

(→**1**) with acetyl chloride to finally obtain the desired three-picket porphyrin **3a** by addition of 3-quinoline acyl chloride. Iron insertion in the porphyrin leaves the second site of metallation free for copper(I) complexation, which represents the last step before addition of a 100- to 1000-fold excess of the nitrogenous base (1,2-dimethylimidazole) to stabilize the iron(II) center as a five-coordinate complex. To compare[6] the effect of an intramolecular base, the analogous complex with a tailed base, **4a**, was synthesized starting from the recently described monoprotected trityl porphyrin **2** (Scheme 1).[7] Grafting of quinolinoyl pickets is followed by deprotection of the trityl group, leading to an open face of the porphyrin, which can be functionalized at will. As first described by Chang and Young,[8] 3-chloromethylbenzoyl chloride was used to link imidazole or 2-methylimidazole to the porphyrin.[9]

Electrochemical studies with a rotating electrode[10] were carried out to compare the catalytic activity of the newly synthesized compounds. The primary goal of this investigation was to shed light on the role of the copper cation bound to the distal nitrogenous site, more precisely to know if its presence is essential for the catalytic $4e^-$ reduction of O_2 to H_2O. The second motivation for this comparison was to examine the part played by the *N*-base, the axial ligand of the iron of the porphyrin, and particularly if this base is more efficient when attached to the macrocycle. The compounds reported in the present study, like other models already described in the literature, bind dioxygen reversibly in aprotic solvents when only a five-coordinate iron(II) center is present. Under identical experimental conditions, when copper(I) is bound to the distal nitrogenous site, the dioxygen fixation is irreversible, which suggests that O_2 interacts with the two metal centers.[4a] The activity for the reduction of O_2 has been tested with catalysts adsorbed onto highly ordered graphite electrodes (edge-plane graphite electrode, EPGE), in contact with an aqueous solution at an acidity level close to the physiological pH value, at which cytochrome *c* oxidase operates as a $4e^-$ catalyst.[1]

The reduction of O_2 at an electrode modified with the Fe – Cu complex **3c** begins at 0.15 V vs. SCE (Figure 2, curve b). From the comparison with the $2e^-$ reduction wave on bare EPGE, the

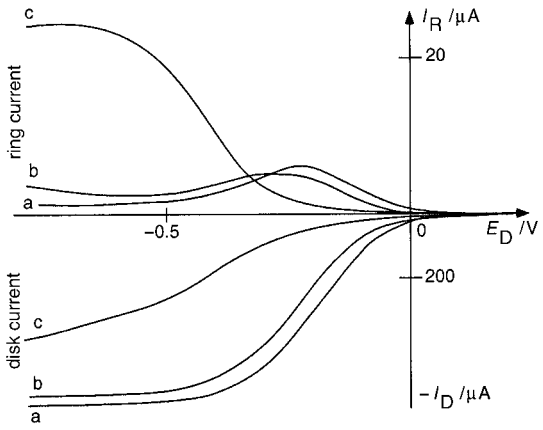

Figure 2. *Rotating-ring – disk voltammetry for O_2 reduction. The graphite disk was impregnated with **3b** (curve a) or **3c** (curve b), 1,2-dimethylimidazole was used as an exogenous base. For recording curve c, a bare graphite electrode (EPGE) was used. (pH = 6.86, rotational speed = 100 rpm, SCE as reference electrode, pO_2 = 1 atm, potential of the platinum ring electrode = 0.8 V.) At the disk, dioxygen is reduced to water or hydrogen peroxide; hydrogen peroxide produced at the disk is oxidized when reaching the ring.*

number of electrons exchanged per O_2 molecule is 3.4 – 3.3. H_2O_2 is detected through its oxidation, as soon as O_2 is reduced, from the current rise at the platinum electrode encompassing the graphite disk. This means that the $2e^-$ and $4e^-$ reduction mechanisms occur simultaneously; however, the production of H_2O_2 is higher, at about the half-wave potential for the O_2 reduction, in the activation region of this process. Unfortunately, the catalyst is rapidly degraded by H_2O_2, as proved by consecutive scans, so that the apparent number of electrons for the electrocatalytic reduction is only an approximate figure. Nevertheless, much of O_2 reaching the electrode by diffusion is reduced through the $4e^-$ mechanism. The compound without copper, **3b**, is also a mixed $2e^-/4e^-$ catalyst for the electroreduction of O_2, with the apparent number of electrons exchanged per O_2 molecule even higher (ca. 3.5) than for **3c** (Figure 2, curve a). This comparison between the Fe and Fe – Cu complexes and the fact that the iron-only compound is even more efficient than the Fe – Cu derivative, is of considerable importance in the understanding of the catalytic cycle of cytochrome *c* oxidase models. The results obtained with the present series of compounds are somewhat similar to the observations for the tren-capped "Arbor" models:[4c] These iron-

only complexes are better $4e^-$ catalysts than the iron–copper analogues which catalyze both the $2e^-$ and $4e^-$ reductions. There are two possibilities to explain these observations: 1) The copper center does not interfere with the O_2 molecule bound to the iron during the reduction reaction; 2) the labile copper ion of the tris(*N*-base) complex is no longer coordinated when the catalyst adsorbed onto the graphite electrode is in contact with the aqueous solution. It has to be pointed out that in the articles published about compounds similar to the ones of the present study[4a,g] no proof of the presence of copper in the molecules adsorbed onto the working electrode has been reported. The quinolinoyl picket molecules described here are not as efficient as the tren-capped porphyrins examined earlier;[4c] however, the essential structural parameter for the $4e^-$ reduction does not become evident from the comparison of the two series of results.

The experimental results also provide information about the role of the *N*-base as axial ligand of the iron. The catalytic activity of **4b**, **5b**, and **5c**, compounds with a base covalently linked to the iron porphyrin, is shown in Figure 3. If the voltammograms observed with **3b** (Figure 2, curve a) or **4b** (Figure 3, curve a) are

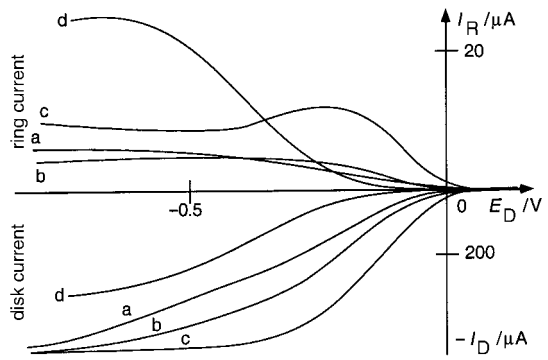

Figure 3. *Rotating-ring–disk voltammetry for O_2 reduction. The graphite disk was impregnated with **4b** (curve a), **5b** (curve b) with a tailed Im base, or **5c** (curve c) with a tailed 2-MeIm base. For recording curve d, a bare graphite electrode (EPGE) was used. (pH = 6.86, rotational speed = 100 rpm, SCE as reference electrode, pO_2 = 1 atm, potential of the platinum ring electrode = 0.8 V.)*

compared, it clearly appears that anchoring an *N*-base as a potential fifth ligand for the iron center does not improve the efficiency of O_2 reduction. From Figures 2 and 3, two categories of catalysts can be distinguished. In the voltammograms of **5c**, **3c**, and **3b**, the intensity of the current for the reduction of O_2 at the graphite disk increases quite steeply. A plateau is reached, which means that the limiting step of the reduction reaction is the mass transport of O_2 in the solution, and not the electron exchange rate (at potentials lower than -0.25 V). However, the slow O_2 transport in solution has to be stressed; the speed of rotation of the electrode (100 rpm) was chosen in order to make sure that in the plateau phase, mass transport would be limiting and, as a consequence, that the current would be proportional to the number of electrons exchanged. For these compounds, the oxidation current of H_2O_2, detected at the platinum ring, increases as soon as the O_2 reduction starts at the modified graphite disk; the production of H_2O_2 reaches a maximum and then decreases. This means that H_2O_2 is produced as soon as O_2 is reduced and that the $4e^-$ reduction is activated more efficiently than the $2e^-$ reduction. In contrast, the reduction current catalyzed by **4b** and **5b** never reaches a plateau. More striking is the fact that even when the reduction current reaches the level observed for **5c** (Figure 3), **3c**, and **3b** (Figure 2), the amount of H_2O_2 produced is lower for the catalysts **4b** and **5b**. One plausible explanation for this observation is that the activation of the two reduction mechanisms ($4e^-$ and $2e^-$) is slower for **4b** and **5b** and that the reduction is limited by the electron exchange rate or the chemical reactions at the electrode. There is no obvious explanation for these observations since Fe and Fe–Cu complexes, with or without a covalently bound axial *N*-ligand, belong to each of the two categories of catalysts. As the kinetics of the catalytic process is limiting, the number of active sites, that is of adsorbed molecules, has certainly a major impact on the reduction. However, positive experimental results for the estimation of the surface concentration of the catalysts on graphite are not available, even differential pulse polarography and square-wave voltammetry failed. Moreover, as stated above, the degradation of the catalysts during the reduction of O_2 is rather rapid so that the surface concentration of the active molecules is certainly not constant during a voltammogram. This degradation also prevents more sophisticated experiments on the kinetics of the electrode reaction, such as a Koutecki–Levich analysis of the O_2 reduction waves.

The compounds reported in the present study, as well as the "Arbor" porphyrins studied earlier, are model compounds of C*c*O that do not have an attached nitrogen base but promote the $4e^-$ reduction of O_2. The role of the copper ion for the catalytic activity is also a matter of debate. Nevertheless, two explanations seem consistent with our observations concerning the quinolinoyl picket porphyrins. The first one has been advanced by Rousseau et al. who have proposed that the copper(I) ion only serves as a pre-storage site for dioxygen, which might bind more rapidly to copper(I) than to iron(II).[11] In that case, the copper ion would not really participate in the catalytic cycle. The second hypothesis has been proposed by Yoshikawa et al. The tyrosine residue (Tyr 244), present on the distal side of the active site of the enzyme, might be involved in catalysis, as its proton could cooperate with the iron ion in the formation of a hydroperoxo complex (Fe^{III}-O-OH) when electrons and protons are supplied. The involvement of the copper ion would lead to an inactive peroxo complex (Fe^{III}-O_2-Cu^{II}) when the electron/proton flow becomes insufficient.[12]

In conclusion, these new picket porphyrins are efficient catalysts for the electroreduction of dioxygen to water, with or without copper in the distal side of the porphyrin and whether or not a tailed nitrogen base stabilizes iron(II) as a five-coordinate complex. To our knowledge, this is the first time that such comparisons have been made to find out precisely which features are really necessary to elaborate a functional biomimetic model of C*c*O. From our point of view, this could be a key point in the understanding of the catalytic cycle. These results, together with the study of "Arbor" porphyrins, do not support the formation of a peroxo-bridged Fe—Cu species as the active

  1439-4227/01/02/02 $ 17.50+.50/0 CHEMBIOCHEM **2001**, No. 2

intermediate in the catalytic cycle of our model compounds but are consistent with the formation of an iron-only (peroxo) complex, which may or may not be protonated. It is now clear that the copper ion is not indispensable for the $4e^-$ reduction of oxygen at physiological pH, at which these model compounds are adsorbed onto a graphite electrode. In the enzyme, where many steps such as O_2 or H^+ transport and e^- transfer are different, Cu ions could play an essential role in one of these events. A new generation of compounds is already under investigation to improve our understanding of the important features of the catalytic activity of C*c*O.

Experimental Section

(5α-Acetyl)porphyrin 1: Acetyl chloride (115 μL, 1.1 mmol) was slowly added to a mixture of $\alpha,\alpha,\alpha,\alpha$-5,10,15,20-tetra(*o*-aminophenyl)porphyrin[5] (1 g, 1.48 mmol) dissolved in THF and triethylamine (210 μL, 3.0 mmol) at 0 °C to yield 490 mg (0.68 mmol, 46%) of **1**. ^{1}H NMR (500 MHz, $CDCl_3$, 25 °C): $\delta = 8.96$ (br. s, 4H; Hβ-$_{pry}$); 8.95 (d, $^3J(H,H) = 4.7$ Hz, 2H; Hβ_{pyr}); 8.81 (d, $^3J(H,H) = 4.7$ Hz, 2H; Hβ_{pyr}); 8.73 (d, $^3J(H,H) = 8.0$ Hz, 1H; H_{aro}); 8.01 (d, $^3J(H,H) = 7.5$ Hz, 1H; H_{aro}); 7.89 (d, $^3J(H,H) = 7.5$ Hz, 3H; H_{aro}); 7.86 (t, $^3J(H,H) = 8.0$ Hz, 1H; H_{aro}); 7.64 (t, $^3J(H,H) = 8.0$ Hz, 3H; H_{aro}); 7.53 (t, $^3J(H,H) = 8.0$ Hz, 1H; H_{aro}); 7.22 (t, $^3J(H,H) = 7.5$ Hz, 3H; H_{aro}); 7.15 (d, $^3J(H,H) = 7.5$ Hz, 3H; H_{aro}); 6.82 (s, 1H; NHCO); 3.53 (br. s, 6H; NH_2); 1.27 (s, 3H; CH_3); −2.66 (s, 2H; NH_{pyr}); MS (FAB): *m/z* (%): 716.7 (100) $[M]^{+\bullet}$; elemental analysis (%): calcd for $C_{46}H_{36}N_8O \cdot 2H_2O$: C 73.39, H 5.36, N 14.88; found: C 73.80, H 4.92, N, 15.10.

(5α-Acetyl)-(10,15,20-α,α,α-quinolinoyl-picket)porphyrin 3a: Step i: 3-quinolinecarboxylic acid chloride was prepared starting from the acid (180 mg, 1.04 mmol) by refluxing it overnight in thionyl chloride. The mixture was dried, redissolved in benzene, filtered, and dried again. 170 mg of quinolinecarboxylic acid chloride (0.88 mmol, 85%) was obtained. It was analyzed by ^{1}H NMR spectroscopy in the form of its ethyl ester derivative. ^{1}H NMR (500 MHz, CD_3OD, 25 °C): $\delta = 9.74$ (d, $^4J(H,H) = 1.5$ Hz, 1H; H_{aro}); 9.67 (q, $^4J(H,H) = 2.0$ Hz, 1H; H_{aro}); 8.53 (d, $^3J(H,H) = 8.5$ Hz, 1H; H_{aro}); 8.41 (d, $^3J(H,H) = 8.5$ Hz, $^4J(H,H) = 2.0$ Hz, 1H; H_{aro}); 8.33 (d, $^3J(H,H) = 7.0$ Hz, $^4J(H,H) = 1.5$ Hz, 1H; H_{aro}); 8.09 (d, $^3J(H,H) = 7.0$ Hz, $^4J(H,H) = 1.0$ Hz, 1H; H_{aro}); 4.57 (q, $^3J(H,H) = 7.0$ Hz, 2H; CH_2); 3.62 (t, $^3J(H,H) = 7.0$ Hz, 3H; CH_3). In a 100 mL round-bottom flask equipped with a stirring bar and nitrogen inlet, compound **1** (160 mg, 0.21 mmol) was dissolved in 50 mL of freshly distilled THF and 0.1 mL of dry NEt_3. 3-Quinolinecarboxylic acid chloride (140 mg, 0.74 mmol) dissolved in THF was added over 1 h. After incubation overnight, the mixture was dried, redissolved in CH_2Cl_2, washed with sat. aq $NaHCO_3$, and purified by flash chromatography on a silica gel column. 218 mg of **3a** (0.18 mmol, 88%) were obtained. ^{1}H NMR (500 MHz, $CDCl_3$, 25 °C): $\delta = 9.14$ (d, $^3J(H,H) = 4.7$ Hz, 2H; Hβ_{pyr}); 9.09 (d, $^3J(H,H) = 4.7$ Hz, 2H; Hβ_{pyr}); 8.99 (d, $^3J(H,H) = 4.7$ Hz, 2H; Hβ_{pyr}); 8.86 (d, $^3J(H,H) = 4.7$ Hz, 2H; Hβ_{pyr}); 8.81 (d, $^3J(H,H) = 8.0$ Hz, 2H; H_{aro}); 8.72 (d, $^3J(H,H) = 7.5$ Hz, 1H; H_{aro}); 8.57 (s, 1H; NHCO); 8.48 (d, $^3J(H,H) = 7.5$ Hz, 1H; H_{aro}); 8.24 (d, $^3J(H,H) = 7.5$ Hz, 2H; H_{aro}); 8.18 (d, $^3J(H,H) = 8.0$ Hz, 2H; H_{aro}); 8.03 (s, 2H; NHCO); 7.96 (t, $^3J(H,H) = 8.0$ Hz, 3H; H_{aro}); 7.83 (d, $^3J(H,H) = 7.5$ Hz, 1H; H_{aro}); 7.80 (t, $^3J(H,H) = 7.5$ Hz, 1H; H_{aro}); 7.71 (m, 4H); 7.56 (s, 2H; H_{aro}); 7.47 (t, $^3J(H,H) = 8.0$ Hz, 2H; H_{aro}); 7.34 (s, 2H; H_{aro}); 7.12 (m, 4H); 6.95 (m, 5H); 6.80 (d, $^3J(H,H) = 7.5$ Hz, 1H; H_{aro}); 6.63 (d, $^3J(H,H) = 7.5$ Hz, 2H; H_{aro}); 0.44 (s, 3H; CH_3); −2.37 (s, 2H; NH_{pyr}); UV/Vis (CH_2Cl_2): λ_{max} (ε) = 423 (Soret, 305400), 517 (20400), 551 (6000), 590 (6900), 645 (2900 $mol^{-1}\,dm^3\,cm^{-1}$); HR-MS (liquid secondary ion MS, LSIMS): *m/z* (%): calcd for $C_{76}H_{52}N_{11}O_4$ 1182.4204 $[M+H]^+$, found 1182.4253 (100); elemental analysis (%): calcd for $C_{76}H_{51}N_{11}O_4$: C 77.21, H 4.35, N 13.03; found: C 76.89, H 4.49, N 13.07.

3b: Step vi: In a glove box (dioxygen concentration less than 1 ppm), **3a** (20 mg) was dissolved in THF and heated to 55 °C. Then, ten drops of 2,6-lutidine and a fivefold excess of iron(II) bromide were added. After 5 h the mixture was dried, redissolved in CH_2Cl_2, filtered over a Celite plug, and dried again; yield 90%. ^{1}H NMR (500 MHz, [D_5]pyridine, 50 °C): $\delta = 9.71$ (s, 2H; NHCO); 9.35 (s, 1H; NHCO), 8.95 (d, $^3J(H,H) = 4.7$ Hz, 2H; Hβ_{pyr}); 8.93 (d, $^3J(H,H) = 4.7$ Hz, 2H; Hβ_{pyr}); 8.90 (d, $^3J(H,H) = 4.7$ Hz, 2H; Hβ_{pyr}); 8.83 (d, $^3J(H,H) = 8.0$ Hz, 3H; H_{aro}); 8.77 (d, $^3J(H,H) = 8.0$ Hz, 1H; H_{aro}); 8.74 (d, $^3J(H,H) = 4.7$ Hz, 2H; Hβ_{pyr}); 8.53 (d, $^4J(H,H) = 2.0$ Hz, 2H; H_{aro}); 8.45 (s, 2H); 8.39 (s, 1H); 8.27 (d, $^4J(H,H) = 2.0$ Hz, 1H; H_{aro}); 8.16 (d, $^3J(H,H) = 7.5$ Hz, 1H; H_{aro}); 8.02 (d, $^3J(H,H) = 7.5$ Hz, 1H; H_{aro}); 7.79 (m, 6H); 7.70 (m, 3H); 7.50 – 7.43 (m, 8H); 7.38 – 7.28 (m, 6H); 0.87 (s, 3H; CH_3); HR-MS (LSIMS): *m/z* (%): calcd for $C_{76}H_{50}N_{11}O_4Fe$ 1236.3397 $[M+H]^+$, found 1236.3382 (100). The reversible oxygenation of the iron(II) complex stabilized by 1,2-dimethylimidazole was verified by UV/Vis spectroscopy.

3c: Step vii: In a glove box, **3b** was dissolved in CH_3CN and refluxed. CuBr was added in excess and heating was continued for 12 h. After filtration of the salt, a 100- to 1000-fold excess of the nitrogen base (1,2-dimethylimidazole) was added to stabilize the complex. Insertion of copper was verified by EPR measurements at 100 K comparing the oxidized form of the complex **3b**, which is characterized by its classical high-spin iron(III) porphyrin signal centered at $g = 6$, and the oxidized form of **3c**, which did not exhibit any signal at 100 K. This feature, already observed with other model compounds, is explained by an antiferromagnetic coupling between the two metal centers. The irreversible oxygenation of the iron(II) – copper(I) species was then observed by UV/Vis spectroscopy.

(5β-Im)-(10,15,20-α,α,α-quinolinoyl-picket)porphyrin 4a: Step i: The same procedure used for the synthesis of **3a** was used but starting from the recently described $\beta,\alpha,\alpha,\alpha$-5,10,15,20-tetra(*o*-aminophenyl)porphyrin, of which the amino function at the β position is protected by a trityl group (**2**; 200 mg, 0.22 mmol).[5] 240 mg of (5β-trityl)-(10,15,20-α,α,α-quinolinoyl-picket)porphyrin (0.18 mmol, 80%) were obtained. ^{1}H NMR (500 MHz, [D_5]pyridine, 25 °C): $\delta = 10.51$ (s, 1H; NHCO); 10.48 (s, 2H; NHCO); 9.23 (d, $^3J(H,H) = 4.7$ Hz, 2H; Hβ_{pyr}); 9.20 (d, $^3J(H,H) = 4.7$ Hz, 2H; Hβ_{pyr}); 9.16 (d, $^3J(H,H) = 4.7$ Hz, 2H; Hβ_{pyr}); 9.10 (d, $^3J(H,H) = 4.7$ Hz, 2H; Hβ_{pyr}); 8.88 (d, $^3J(H,H) = 8.0$ Hz, 2H; H_{aro}); 8.67 (d, $^3J(H,H) = 8.0$ Hz, 1H; H_{aro}); 8.53 (d, $^4J(H,H) = 1.5$ Hz, 1H; H_{aro}); 8.49 (br. s, 2H); 8.36 (d, $^3J(H,H) = 7.5$ Hz, 1H; H_{aro}); 8.27 (m, 3H); 8.08 (br. s, 1H); 7.96 (m, 3H); 7.88 (br. s, 2H); 7.72 (m, 3H); 7.58 (d, $^3J(H,H) = 7.5$ Hz, 1H; H_{aro}); 7.41 (d, $^3J(H,H) = 8.0$ Hz, 2H; H_{aro}); 7.35 (d, $^4J(H,H) = 1.0$ Hz, 1H; H_{aro}); 7.25 (m, 7H); 7.12 (t, $^3J(H,H) = 7.5$ Hz, 2H; H_{aro}); 7.04 (t, $^3J(H,H) = 7.5$ Hz, 1H; H_{aro}); 6.94 – 6.81 (m, 15H); 6.71 (d, $^3J(H,H) = 8.0$ Hz, 2H; H_{aro}); −2.59 (s, 2H; NH_{pyr}); MS (FAB): *m/z* (%): 1382.6 (100) $[M+H]^+$. Step ii: By reacting the product of step i with TFA in CH_2Cl_2, 190 mg of (5β-amino)-(10,15,20-α,α,α-quinolinoyl-picket)porphyrin (0.17 mmol, 95%) were obtained. ^{1}H NMR (500 MHz, $CDCl_3$, 25 °C): $\delta = 9.09$ (d, $^3J(H,H) = 4.7$ Hz, 2H; Hβ_{pyr}); 9.07 (d, $^3J(H,H) = 4.7$ Hz, 2H; Hβ_{pyr}); 8.99 (d, $^3J(H,H) = 4.7$ Hz, 2H; Hβ_{pyr}); 8.91 (d, $^3J(H,H) = 4.7$ Hz, 2H; Hβ_{pyr}); 8.84 (d, $^3J(H,H) = 8.0$ Hz, 1H; H_{aro}); 8.67 (d, $^3J(H,H) = 7.5$ Hz, 2H; H_{aro}); 8.48 (s, 1H); 8.42 (d, $^3J(H,H) = 7.5$ Hz, $^4J(H,H) = 1.0$ Hz, 2H; H_{aro}); 8.21 (d, $^3J(H,H) = 7.5$ Hz, $^4J(H,H) = 1.5$ Hz, 1H; H_{aro}); 8.04 (d, $^4J(H,H) = 2.0$ Hz, 2H; H_{aro}); 7.99 – 7.95 (m, 4H); 7.75 (t, $^3J(H,H) = 7.5$ Hz, $^4J(H,H) = 1.5$ Hz, 3H; H_{aro}); 7.71 (t, $^3J(H,H) = 7.5$ Hz, $^4J(H,H) = 1.0$ Hz, 2H; H_{aro}); 7.47 (t, $^3J(H,H) = 7.5$ Hz, $^4J(H,H) = 1.5$ Hz, 1H; H_{aro}); 7.44 (d, $^4J(H,H) = 2.0$ Hz , 1H; H_{aro}); 7.31 (d, $^3J(H,H) = 7.5$ Hz, $^4J(H,H) = 1.0$ Hz, 1H; H_{aro}); 7.13 (m, 1H); 7.00 (d, $^3J(H,H) = 7.5$ Hz, 1H; H_{aro}); 6.99 – 6.94 (m, 2H); 6.84 (t, $^3J(H,H) = 7.5$ Hz, $^4J(H,H) = 1.0$ Hz, 1H; H_{aro}); 6.76 (m, 8H); 6.33 (br. s, 3H;

NHCO); 5.37 (br. s, 2H; NH_2); −2.28 (s, 2H; NH_{pyr}); MS (FAB): *m/z* (%): 1139.9 (100) $[M]^{+\bullet}$. Step iii: By reacting the product of step ii with 3-chloromethylbenzoyl chloride in THF and NEt_3, 130 mg of (5β-chlorobenzyl)-(10,15,20-α,α,α-quinolinoyl-picket)porphyrin (0.10 mmol, 60%) were obtained. ^{1}H NMR (500 MHz, $CDCl_3$, 50 °C): δ = 9.09 (d, ^3J(H,H) = 4.7 Hz, 2H; Hβ_{pyr}); 9.07 (d, ^3J(H,H) = 4.7 Hz, 2H; Hβ_{pyr}); 8.99 (d, ^3J(H,H) = 4.7 Hz, 2H; Hβ_{pyr}); 8.85 (d, ^3J(H,H) = 4.7 Hz, 2H; Hβ_{pyr}); 8.78 (d, ^3J(H,H) = 8.0 Hz, 1H; H_{aro}); 8.76 (d, ^3J(H,H) = 8.0 Hz, ^4J(H,H) = 1.5 Hz, 1H; H_{aro}); 8.70 (d, ^3J(H,H) = 8.0 Hz, 2H; H_{aro}); 8.34 (m, 3H); 8.17 (d, ^3J(H,H) = 7.5 Hz, ^4J(H,H) = 1.5 Hz, 1H; H_{aro}); 7.99 – 7.93 (m, 5H); 7.86 (br. s, 2H); 7.78 (t, ^3J(H,H) = 8.0 Hz, ^4J(H,H) = 1.5 Hz, 1H; H_{aro}); 7.73 – 7.69 (m, 4H); 7.60 (d, ^3J(H,H) = 7.5 Hz, 1H; H_{aro}); 7.50 (m, 1H); 7.32 – 7.39 (m, 3H); 7.05 (d, ^3J(H,H) = 8.0 Hz, 1H; H_{aro}); 7.00 (t, ^3J(H,H) = 7.5 Hz, 1H; H_{aro}); 6.95 (t, ^3J(H,H) = 7.5 Hz, 1H; H_{aro}); 6.91 – 6.81 (m, 6H); 6.56 m, 2H); 6.46 (br. s, 2H); 6.43 (t, ^3J(H,H) = 7.5 Hz, ^4J(H,H) = 1.5 Hz, 1H; H_{aro}); 6.24 (s, 1H); 5.53 (d, ^3J(H,H) = 8.0 Hz, 2H; H_{aro}); 3.44 (s, 2H; CH_2); −2.19 (s, 2H; NH_{pyr}); MS (FAB): *m/z* (%): 1291.4 (100) $[M]^{+\bullet}$. Step iv: By reacting the product of step iii with imidazole (Im) and NaI in THF at 60 °C in the dark, 20 mg of (5β-Im)-(10,15,20-α,α,α-quinolinoyl-picket)porphyrin (0.015 mmol, 30%) were obtained. ^{1}H NMR (500 MHz, $CDCl_3$, 50 °C): δ = 9.09 (d, ^3J(H,H) = 4.7 Hz, 2H; Hβ_{pyr}); 9.07 (d, ^3J(H,H) = 4.7 Hz, 2H; Hβ_{pyr}); 9.01 (d, ^3J(H,H) = 4.7 Hz, 2H; Hβ_{pyr}); 8.85 (d, ^3J(H,H) = 4.7 Hz, 2H; Hβ_{pyr}); 8.79 (d, ^3J(H,H) = 8.0 Hz, 1H; H_{aro}); 8.74 (d, ^3J(H,H) = 8.0 Hz, 1H; H_{aro}); 8.69 (d, ^3J(H,H) = 8.0 Hz, 2H; H_{aro}); 8.29 (d, ^3J(H,H) = 7.5 Hz, ^4J(H,H) = 1.5 Hz, 2H; H_{aro}); 8.25 (s, 1H); 8.17 (d, ^3J(H,H) = 7.5 Hz, ^4J(H,H) = 1.5 Hz, 1H; H_{aro}); 8.00 – 7.94 (m, 4H); 7.90 (br. s, 2H); 7.79 (m, 2H); 7.72 (t, ^3J(H,H) = 7.5 Hz, ^4J(H,H) = 1.5 Hz, 3H; H_{aro}); 7.60 (d, ^3J(H,H) = 7.5 Hz, ^4J(H,H) = 1.5 Hz, 1H; H_{aro}); 7.43 (m, 1H); 7.30 (t, ^3J(H,H) = 7.5 Hz, ^4J(H,H) = 1.5 Hz, 1H; H_{aro}); 7.07 (d, ^3J(H,H) = 7.5 Hz, ^4J(H,H) = 2.0 Hz, 1H; H_{aro}); 7.01 – 6.93 (m, 4H); 6.88 (t, ^3J(H,H) = 7.5 Hz, ^4J(H,H) = 1.5 Hz, 2H; H_{aro}); 6.82 (d, ^3J(H,H) = 8.0 Hz, 1H; H_{aro}); 6.74 (s, 1H); 6.53 (d, ^3J(H,H) = 7.0 Hz, ^4J(H,H) = 1.5 Hz, 1H; H_{aro}); 6.50 – 6.42 (m, 5H); 6.56 (m, 2H); 6.38 (d, ^3J(H,H) = 8.0 Hz, ^4J(H,H) = 1.0 Hz, 1H; H_{aro}); 6.36 (m, 1H); 6.27 (m, 1H); 5.61 (t, ^4J(H,H) = 1.0 Hz, 1H; H_{aro}); 5.57 (d, ^3J(H,H) = 8.0 Hz , 2H; H_{aro}); 3.95 (s, 2H; CH_2); −2.19 (s, 2H; NH_{pyr}); HR-MS (LSIMS): *m/z* (%): calcd for $C_{85}H_{57}N_{13}O_4Na$ 1346.4554 $[M+Na]^+$, found 1346.4554 (100).

(5β-2-MeIm)-(10,15,20-α,α,α-quinolinoyl-picket)porphyrin 5a: Steps i – iii are identical to those described for the synthesis of **4a**. Step v: By reacting the product of step iii with 2-methylimidazole and NaI in THF at 60 °C in the dark, 40 mg of **5a** (0.03 mmol, 60%) were obtained. ^{1}H NMR (500 MHz, $CDCl_3$, 50 °C): δ = 9.10 (d, ^3J(H,H) = 5.0 Hz, 2H; Hβ_{pyr}); 9.07 (d, ^3J(H,H) = 5.0 Hz, 2H; Hβ_{pyr}); 9.03 (d, ^3J(H,H) = 5.0 Hz, 2H; Hβ_{pyr}); 8.87 – 8.82 (m, 3H); 8.73 (d, ^3J(H,H) = 8.3 Hz, 1H; H_{aro}); 8.64 (d, ^3J(H,H) = 8.0 Hz, 2H; H_{aro}); 8.47 (s, 1H); 8.33 (d, ^3J(H,H) = 7.6 Hz, ^4J(H,H) = 1.1 Hz, 2H; H_{aro}); 8.20 (d, ^3J(H,H) = 7.6 Hz, ^4J(H,H) = 1.1 Hz, 1H; H_{aro}); 8.11 (d, ^4J(H,H) = 1.7 Hz, 1H; H_{aro}); 8.01 – 7.94 (m, 4H); 7.79 – 7.71 (m, 5H); 7.53 (d, ^3J(H,H) = 7.6 Hz, ^4J(H,H) = 1.1 Hz, 1H; H_{aro}); 7.34 – 7.25 (m, 4H); 7.18 (d, ^3J(H,H) = 8.0 Hz, 1H; H_{aro}); 7.01 – 6.91 (m, 2H); 6.75 (m, 4H); 6.68 (d, ^3J(H,H) = 8.3 Hz, 2H; H_{aro}); 6.46 – 6.34 (m, 4H); 6.29 (m, 2H); 6.21 (s, 1H); 5.67 (m, 3H); 3.91 (s, 2H; CH_2); 1.58 (s, 3H; CH_3); −2.34 (s, 2H; NH_{pyr}).

5d: By reacting **5a** (20 mg, 0.015 mmol) with CuBr in MeOH at 50 °C and then with 1 M HCl, 20 mg (0.014 mmol, 95%) of **5d** were obtained. UV/Vis (CH_2Cl_2): λ_{max} (ε) = 428 (Soret, 228 300), 478 (4400), 550 (20 200), 595 (2200 $mol^{-1}\,dm^3\,cm^{-1}$); MS (MALDI-TOF, linear mode): *m/z* (%): 1398.7 (100) $[M]^{+\bullet}$; elemental analysis (%): calcd for $C_{87}H_{59}N_{13}O_4Cu\cdot CH_2Cl_2\cdot CH_3OH$: C 69.67, H 4.19, N 12.00; found. C 69.54, H 3.94, N 11.64. Steps vi and vii are identical to those described for the synthesis of **3b** and **3c**, without the need for stabilization of the compounds with an exogenous base.

Electrochemical studies: The diameter of the edge-plane graphite electrode was 6 mm; the collecting efficiency of the ring-disk electrode was 27% (Pine Instrument Co.). The graphite electrode is modified by dipping it for 5 min in the solution of the catalyst in $CHCl_3$. A bipotentiostat (Solea-Tacusel) pilots the disk potential, whereas the platinum ring is maintained at 0.8 V vs. SCE for experiments in a phosphate buffer (0.025 M KH_2PO_4, 0.025 M Na_2HPO_4, pH 6.86).

[1] a) B. G. Malmström, *Chem. Rev.* **1990**, *90*, 1247 – 1260; b) M. X. Calhoun, J. W. Thomas, R. Gennis, *Trends Biochem. Sci.* **1994**, 325 – 330; c) R. Gennis, S. Ferguson-Miller, *Science* **1995**, *269*, 1063 – 1064; d) S. Ferguson-Miller, G. T. Babcock, *Chem. Rev.* **1996**, *96*, 2889 – 2907.

[2] a) C. Varotsis, Y. Zhang, E. H. Appelman, G. T. Babcock, *Proc. Natl. Acad. Sci. USA* **1993**, *90*, 237 – 241; b) C. Varotsis, G. T. Babcock, *J. Am. Chem. Soc.* **1995**, *117*, 11 260 – 11 269; c) T. Kitagawa, T. Ogura in *Progress in Inorganic Chemistry, Vol. 45* (Ed.: K. D. Karlin), Wiley, New York, **1997**, pp. 431 – 479.

[3] a) T. Tsukihara, H. Aoyama, E. Yamashita, T. Tomizaki, H. Yamaguchi, K. Shinzawa-Itoh, R. Nakashima, R. Yaono, S. Yoshikawa, *Science* **1995**, *269*, 1069 – 1074; b) S. Iwata, C. Ostermeier, B. Ludwig, H. Michel, *Nature* **1995**, *376*, 660 – 669; c) T. Tsukihara, H. Aoyama, E. Yamashita, T. Tomizaki, H. Yamaguchi, K. Shinzawa-Itoh, R. Nakashima, R. Yaono, S. Yoshikawa, *Science* **1996**, *272*, 1136 – 1144.

[4] a) J. P. Collman, L. Fu, P. C. Herrmann, X. M. Zhang, *Science* **1997**, *275*, 949 – 951; b) B. Andrioletti, D. Ricard, B. Boitrel, *New J. Chem.* **1999**, *23*, 1143 – 1150; c) D. Ricard, B. Andrioletti, M. L'Her, B. Boitrel, *Chem. Commun.* **1999**, 1523 – 1524; d) H. V. Obias, G. P. F. van Strijdonck, D. H. Lee, M. Ralle, N. J. Blackburn, K. D. Karlin, *J. Am. Chem. Soc.* **1998**, *120*, 9696 – 9697; e) F. Tani, Y. Matsumoto, Y. Tachi, T. Sasaki, Y. Naruta, *Chem. Commun.* **1998**, 1731 – 1732; f) T. Sasaki, Y. Naruta, *Chem. Lett.* **1995**, 663 – 664; g) J. P. Collman, M. Rapta, M. Broring, L. Raptova, R. Schwenninger, B. Boitrel, L. Fu, M. L'Her, *J. Am. Chem. Soc.* **1999**, *121*, 1387 – 1388.

[5] a) J. P. Collman, R. R. Gagne, T. R. Halbert, J.-C. Marchon, C. A. Reed, *J. Am. Chem. Soc.* **1973**, *95*, 7868 – 7870; b) J. P. Collman, R. R. Gagne, C. A. Reed, T. R. Halbert, G. Lang, W. T. Robinson, *J. Am. Chem. Soc.* **1975**, *97*, 1427 – 1439.

[6] This structural feature has been described as being essential to obtain the $4e^-$ reduction of dioxygen, leading to difficult, specific, and long-step syntheses, whereas efficient and selective $4e^-$ catalysts can be obtained by much shorter and straightforward synthetic pathways.

[7] J. P. Collman, M. Bröring, L. Fu, M. Rapta, R. Schwenninger, A. Straumanis, *J. Org. Chem.* **1998**, *63*, 8082 – 8083.

[8] R. Young, C. K. Chang, *J. Am. Chem. Soc.* **1985**, *107*, 898 – 909.

[9] As in the case of the picket-fence porphyrin (for more details, see J. P. Collman, C. A. Reed, *J. Am. Chem. Soc.* **1973**, *95*, 2048 – 2049), we have also employed 2-methylimidazole to avoid the eventual formation of a six-coordinate complex with the axial base.

[10] This has been studied by rotating-ring – disk voltammetry after adsorbtion onto an edge-plane graphite electrode (EPGE), a disk surrounded by a platinum ring. The potential of the ring is maintained at a suitable value to detect (through its oxidation) H_2O_2 possibly produced at the disk by a $2e^-$ process. From comparison with the dioxygen reduction on bare EPGE, which is a purely $2e^-$ process, the number of electrons exchanged per O_2 molecule can be estimated.

[11] D. L. Rousseau, S. H. Han, S. H. Song, Y. C. Ching, *J. Raman Spectrosc.* **1992**, *23*, 551 – 556.

[12] S. Yoshikawa, K. Shinzawa-Itoh, R. Nakashima, R. Yaono, E. Yamashita, N. Inoue, M. Yao, M. J. Fei, C. P. Libeu, T. Mizushima, H. Yamaguchi, T. Tomizaki, T. Tsukihara, *Science* **1998**, *280*, 1723 – 1729.

[13] To avoid any confusion, a classical α,β nomenclature has been used[5] to refer to substituents on one side of the porphyrin ring as α, whereas β refers to the other side. For example, compound **1** is named (5α-monoacetyl)porphyrin. That means that the picket fastening the C5 atom of the porphyrin ring is functionalized with an acetyl group on one side of the macrocycle.

Received: June 19, 2000
Revised version: September 13, 2000 [Z80]

